

Innovative Materials for Aircraft Morphing

J. O. Simpson, S. A. Wise, R. G. Bryant, R. J. Cano, T. S. Gates,
J.A. Hinkley, R.S. Rogowski, and K. S. Whitley

Materials Division
NASA Langley Research Center
Hampton, VA 23681

ABSTRACT

Reported herein is an overview of the research being conducted within the Materials Division at NASA Langley Research Center on the development of smart material technologies for advanced airframe systems. The research is a part of the Aircraft Morphing Program which is a new six-year research program to develop smart components for self-adaptive airframe systems. The fundamental areas of materials research within the program are computational materials; advanced piezoelectric materials; advanced fiber optic sensing techniques; and fabrication of integrated composite structures. This paper presents a portion of the ongoing research in each of these areas of materials research.

KEYWORDS

computational materials, piezoelectrics, ceramics, polymers, fiber optics, composite fabrication, sensors, actuators

1. INTRODUCTION

The Aircraft Morphing program¹ at NASA Langley Research Center (LaRC) is a fundamental research program to develop and mature smart component technologies for advanced airframe systems. The ultimate objective is to provide active component technologies that enable self-adaptive flight for revolutionary improvements in performance and safety in a cost-effective manner. Within the Materials Division (MD) advanced materials are being developed for sensors and actuators, as well as polymers for integrating smart devices into composite structures. As shown in Figure 1, MD contributions to the Aircraft Morphing Program reside in four key areas: computational materials; advanced piezoelectric materials; fiber optic sensing devices and integrated composite structures.

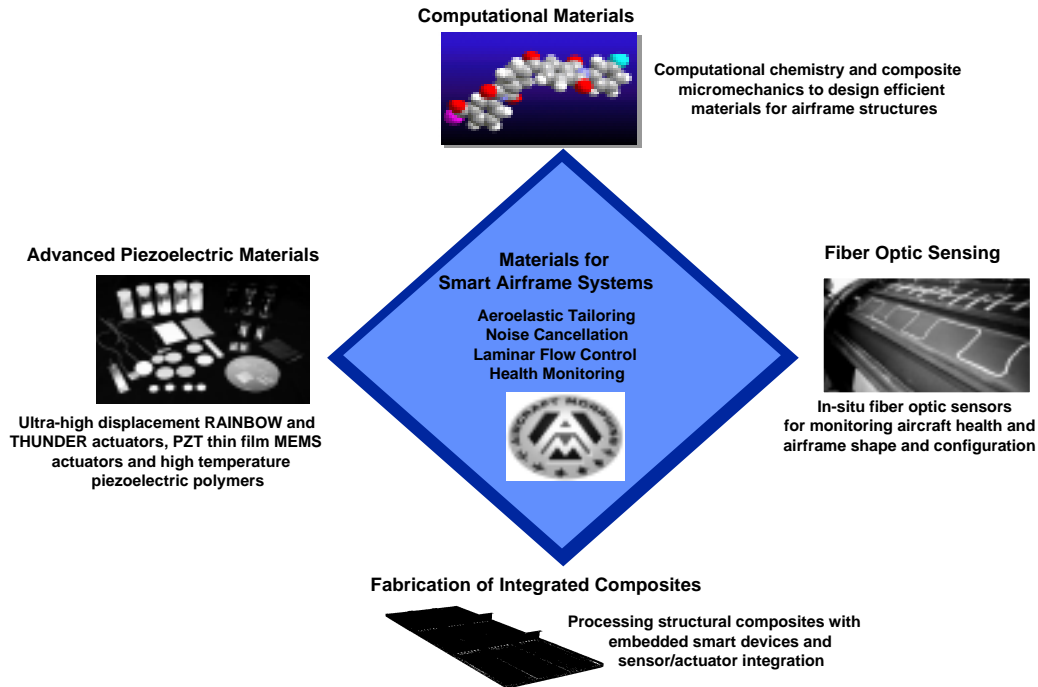


Figure 1. Materials research areas for smart airframe systems.

The computational materials effort is focused on developing predictive tools for the efficient design of new materials with the appropriate combination of properties for next generation smart airframe systems. Research in the area of advanced piezoelectrics includes optimizing the efficiency, force output, use temperature, and energy transfer between the structure and device for both ceramic and polymeric materials. For structural health monitoring, advanced non-destructive techniques including fiber optics are being developed for detection of delaminations, cracks and environmental deterioration in aircraft structures. Methods of confirming aerodynamic shape of a conformable structure and measuring air flow characteristics with fiber optic sensors are also a part of this program. Lastly, innovative fabrication techniques for processing structural composites with sensor and actuator integration are being developed. A majority of this research will be completed for specific applications including the fabrication of a composite panel with embedded shape memory alloys (SMA) for reducing sonic fatigue in aircraft structures. The research in each of these key areas has been designed to meet application needs of the Aircraft Morphing program including aeroelastic tailoring, noise cancellation, laminar flow control and airframe health monitoring. Within this paper, a portion of the ongoing research in each of the areas of materials research is highlighted.

2. COMPUTATIONAL MATERIALS

Developments in a number of areas of aeronautics are currently materials-limited. These areas include the creation of efficient, lightweight structures, some aspects of propulsion, noise and vibration abatement, and active controls. Recent, rapid increases in computer power and improvements in computational techniques open the way to the use of simulations in the development of new materials. At NASA-LaRC, computer-aided design of materials has concentrated on two classes of materials: high performance continuous-fiber reinforced polymer matrix composites and piezoelectric films from high temperature polyimides.

An integrated, predictive computer model is being developed to bridge the microscopic and macroscopic descriptions of polymer composites. This model will significantly reduce development costs by bringing physical and microstructural information into the realm of the design engineer. The range of length and time scales involved is huge, and different scientific and engineering disciplines are involved as shown in Table 1. Models at each level require experimental verification and must connect with models at adjacent levels.

Table 1. Interdisciplinary Nature of Material Modeling

Level	Discipline	Inputs	Outputs
Quantum	Theoretical Chemistry	Atomic Structure	Molecular Structure & Energetics
Nano	Polymer Physics	Molecular Structure	PVT Behavior (Equation of State), Transport Properties
Meso	Micro-mechanics	Constituent Properties	Lamina Properties, Constitutive Behavior
Macro	Continuum Mechanics	Lamina Properties	Laminate Engineering Properties

As an example, at the meso level, constitutive models can be based upon concepts of composite micromechanics combined with mathematical descriptions of the properties of the fiber and matrix constituents. Experiments provide insights into the proper form of the analytical description as well as the material properties required for the selected model. An analytical micromechanics model has been developed to predict the nonlinear stress/strain behavior of advanced composites at elevated temperatures². The model is based upon a square array with the fiber and matrix regions represented by rectangular sections. The fiber is assumed linear elastic and the matrix is assumed to be a nonlinear, orthotropic material. A one-parameter potential function is used in the flow rule to predict the plastic strain during loading. Material properties of the fiber and matrix were measured in the laboratory and used as inputs to the model. Figure 2 shows the predicted stress/strain response of the IM7/5260 unidirectional composite material for varying degrees of off-axis loading. Experimental test data compares favorably to the predictions for several of the off-axis angles.

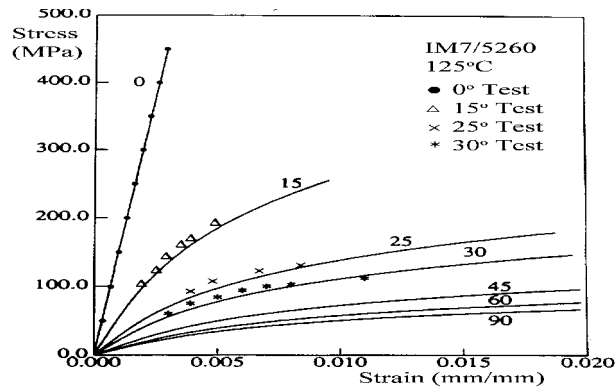


Figure 2. Composite test data versus micromechanics model predicted behavior of IM7/5260 material at 125°C. Test data represents measured stress/strain response for 4 different off-axis, unidirectional specimens.

3. ADVANCED PIEZOELECTRIC MATERIALS

3.1 Piezoelectric Polymers

A research problem that combines both computational and experimental studies is the development of high performance, piezoelectric polymeric materials. The piezoelectric response of a polymer is a function of its dipole concentration, the degree of dipole orientation, and the mechanical properties of the polymer. Currently, fluoropolymers such as polyvinylidene fluoride (PVDF) are the state of the art in piezoelectric polymers. The development of other classes of piezoelectric polymers could provide enabling materials technology for a variety of aerospace and commercial applications. Polyimides are of particular interest due to their high temperature stability and the ease with which various polar pendant groups may be incorporated³. Particularly interesting for the Aircraft Morphing program is the potential use of piezoelectric polyimides in MEMS devices as fluoropolymers do not possess the chemical resistance or thermal stability necessary to withstand conventional MEMS processing. Described herein is an overview of the computational and experimental research that has been completed for an amorphous polyimide with pendant, polar cyano groups in the polymer backbone.

In order to induce a piezoelectric response, the polymer is poled by applying an electric field ($E_p = 100$ MV/m) across the thickness of the polymer at an elevated temperature sufficient to allow mobility of the molecular dipoles. The dipoles are aligned with the applied field and will partially retain the induced polarization when the temperature is lowered below the glass transition temperature in the presence of the field. The resulting remanent polarization is proportional to the level of piezoelectricity.

To computationally simulate the experimental poling process, semi-empirical molecular orbital calculations on model segments of the polymers were used to obtain the electron distributions and potential energy surfaces of the segments. Calculated dipole moments of the model segments were compared with experimental data whenever possible. In addition, the torsional barriers were of interest because they dictate the flexibility of the polymer backbone and hence the ability of the dipoles to orient in response to an external field. A modified force field for use in molecular dynamics simulations was then created. A five unit long polymer was built and packed into a cell with three-dimensional periodic boundary conditions at the experimental density. The temperature and electric field were scaled to bring the poling response into the simulation timescale (200 picoseconds.) From this model, dielectric relaxation strengths were calculated which are in excellent agreement with experimental results, indicating that the computational model can be used as a reliable tool to guide the synthesis of new piezoelectric polymers⁴.

Figure 3 presents measured piezoelectric properties, d_{31} , as a function of temperature for the NASA experimental polyimide and state of the art, PVDF. The piezoelectric coefficient for the polyimide increases with temperature and extends well beyond the feasible temperature range of use for PVDF. However, its piezoelectric response is an order of magnitude lower than that of PVDF. Ongoing research, guided by computational models, should provide improved understanding of the requirements for heightened piezoelectric response and the ability to rapidly evaluate candidate structures in consultation with synthetic polymer chemists.

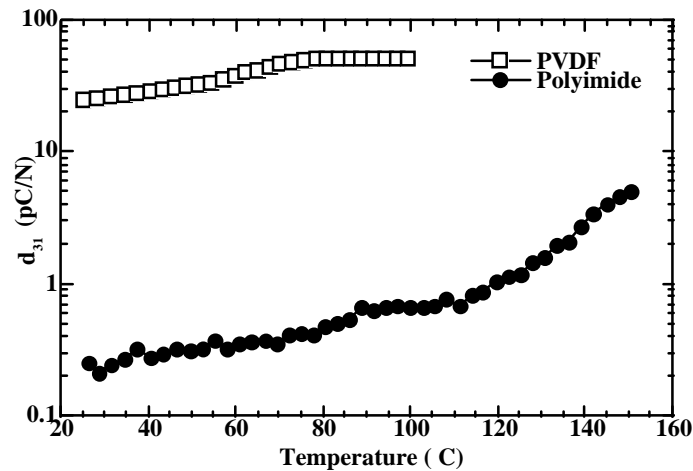


Figure 3. Piezoelectric coefficient as a function of temperature for polyimide and PVDF.

3.2 High-Displacement Piezoelectric Ceramic Actuators

Piezoelectric devices have been identified as a promising actuator technology for the implementation of active boundary layer control, high bandwidth noise suppression and aeroservoelastic tailoring. However, many potential aerospace applications require displacement performance larger than what is achievable in conventional piezoelectrics. Recently LaRC MD researchers have developed two high-displacement piezoelectric actuator technologies, RAINBOW (Reduced And Internally-Biased Oxide Wafer) and THUNDER (THin layer composite UNimorph ferroelectric DrivER and sensor) to meet these requirements. These devices are unimorph-type actuators which consist of a piezoelectric ceramic layer bonded to one or more non-piezoelectric secondary layers. Because of the use of elevated temperatures during processing, internal stresses are created in the structures which significantly enhance displacement through the thickness of the devices. The reader is referred to the literature for more information on RAINBOW⁵⁻⁷ and THUNDER⁸⁻¹⁰ devices and their application.

Currently, the processing and characterization of these high-displacement actuators are under investigation. One recent characterization study involved the effects of electric field, load and frequency on the displacement properties of rectangular THUNDER devices. Results showed that individual actuators were capable of free displacements in excess of 3 mm when tested at ± 9 kV/cm. Increasing device stiffness through metal selection and thickness resulted in improved load-bearing performance at the expense of displacement, allowing devices to be designed with a range of performance capabilities. Figure 4a shows a strain versus voltage curve for a THUNDER device produced with a 0.1-mm thick stainless steel backing and a 0.2-mm thick PZT-5A ceramic layer. In this test, the actuator demonstrated a maximum of 1.7-mm total stroke with no load decreasing to approximately 1-mm total stroke with a 250-g point load. Figure 4b shows the displacement performance as a function of frequency for the same actuator when clamped on one end. The resonance frequency was found to vary significantly with clamping configuration and improved clamping methods are currently being developed application specific mounting configurations.

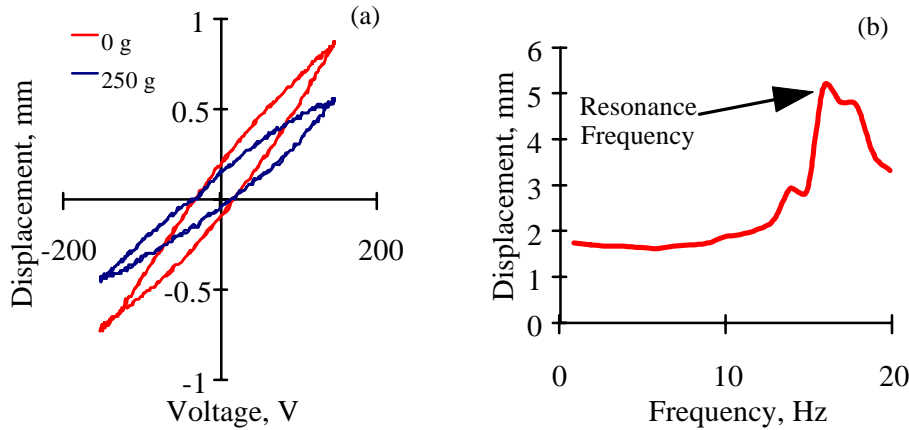


Figure 4. Displacement performance of THUNDER actuator versus voltage (a) and frequency (b).

As many aeronautics applications of high-displacement piezoelectric actuators will require continuous, long-term operation of the devices, the fatigue characteristics of these materials are also under investigation. In these measurements, the displacement and/or polarization properties of the actuators have been evaluated under continuous application of electric fields for more than 10 million cycles. Example performance properties for RAINBOW devices produced from different starting piezoelectric compositions are illustrated in Figure 5a and 5b. Figure 5a shows the normalized free displacement performance of the devices over time, while Figure 5b shows the performance when a 300-g static load was applied during testing. When evaluated without load, the actuator displacement decreased less than 10% over the 10^7 cycles tested. However, noticeable displacement degradation (20-50%) was observed when the RAINBOWs were tested under a 300g static load^{11,12}. To improve these results, researchers are currently evaluating techniques to increase the load-bearing capability of the actuators through both enhanced processing techniques and alternative mounting configurations.

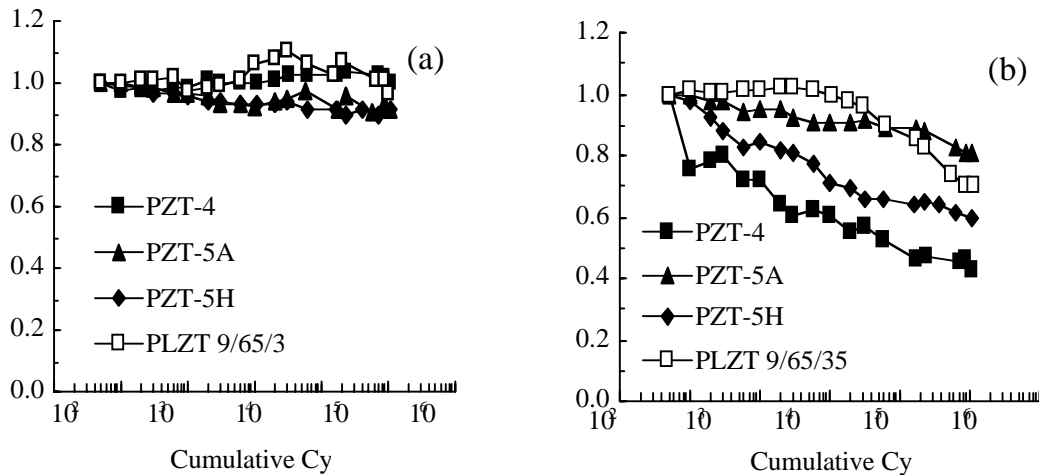


Figure 5. Fatigue characteristics of RAINBOW high-displacement actuators when evaluated under (a) no load and (b) 300-g static load.

3.3 Ferroelectric Thin Films Microactuators

Recent preliminary results¹³ on the integration of ferroelectric thin films with MEMS devices, indicate the feasibility of producing microactuators for application in aerospace systems. PZT-based microactuators (0.2 to 10 μm thick) have demonstrated displacements of 0.1 to 0.6 μm at 5 to 10 V operation¹⁴. To further develop these devices, a metallo-organic decomposition (MOD) process is being used to produce high-quality ferroelectric thin films on Si microstructures.

In this work, piezoelectric 2/53/47 and electrostrictive 9/65/35 solutions were deposited onto platinum-coated silicon (i.e., Pt/Si) and silver foil substrates. The films possessed ferroelectric hysteresis loops similar to the corresponding

bulk ceramics, as shown in Figure 6. The piezoelectric films exhibited remanent polarizations ($P_R = 28.6 \mu\text{C}/\text{cm}^2$), saturation polarizations ($P_{\text{sat}} = 35.1 \mu\text{C}/\text{cm}^2$), and coercive fields ($E_C = 50.7 \text{ kV}/\text{cm}$) commensurate with bulk properties. Displacements of 1 to 10 μm have been demonstrated to date. Current work is underway to fully integrate the ferroelectric films with micromachined silicon diaphragms for use in flow control applications.

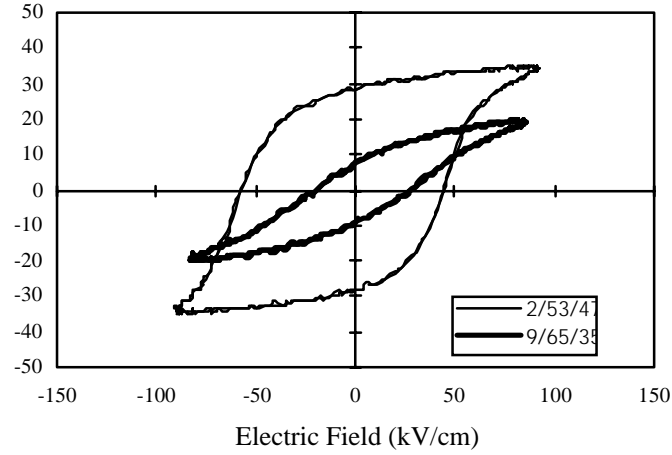


Figure 6. Polarization versus electric field performance of 2/53/47 and 9/65/35 thin films on silver foil.

4. AIRCRAFT HEALTH MONITORING WITH DISTRIBUTED FIBER OPTIC SENSORS

Within the Aircraft Morphing program, fiber optic sensors are being developed for monitoring critical structures on future aircraft which are expected to be largely carbon fiber reinforced composite structures. Methods for embedding the optical fibers in these composites are being investigated. With embedded sensors, composite cure can be monitored leaving the sensors as an integral part of the structure for health monitoring. For structural health monitoring, advanced non-destructive techniques, including optical, thermal, ultrasonic and radiographic, will be developed for detection of delaminations, disbonds, cracks and environmental deterioration in aircraft structures. Continual monitoring of structural well-being will improve aircraft safety and decrease turnaround time and maintenance costs. The main focus is on temperature and strain measurement in a single fiber. Other parameters of interest are aerodynamic quantities such as flow and pressure and conformation of aerodynamic surfaces.

Fiber Optic Distributed Strain Sensor (FODSS)

The FODSS instrument consists of a wavelength-tunable narrow linewidth laser, a fiber optic network containing a sensing fiber with Bragg grating sensors, light detection photodiodes, signal conditioning electronics, and a digital signal processor. Bragg gratings written into an optical fiber by a UV laser can be used as a single point sensor along the length of an optical fiber. NASA LaRC has developed a method for demodulation of over 50 gratings along a 7-m length of fiber for distributed measurement of strain, or hydrogen¹⁵. The Bragg grating sensor reflects only a narrow band of light wavelengths propagating in the fiber. The equation governing the center wavelength of this reflected band is

$$2n\Lambda = \lambda \quad (1)$$

where n is the index of refraction of the fiber core, λ is the reflected wavelength, and Λ is the grating spacing. Strain is defined by the change in length over length, which for a Bragg grating sensor is,

$$\varepsilon \equiv \frac{\Lambda - \Lambda_B}{\Lambda_B} \quad (2)$$

where the subscript **B** refers to a baseline grating spacing value obtained prior to flight. FODSS measures the wavelength of light reflected by a grating to determine its spacing Λ via Equation (1). Therefore in terms of reflected wavelength strain can be written as,

$$\varepsilon = \frac{\lambda - \lambda_B}{\lambda_B} \quad (3).$$

The form of the equation, corrected for material properties, is given by,

$$\varepsilon = K \left(\frac{\lambda - \lambda_B}{\lambda_B} - \xi \Delta T \right) \quad (4)$$

where the constant K is a function of the refractive index, Poisson's ratio, and strain-optic constants of the fiber, ξ is the thermo-optic coefficient, and ΔT is change in temperature.

A block diagram of the FODSS demodulation technique is shown in Figure 7. FODSS detects signals from the low finesse Fabry-Perot cavities formed between each grating and its reference reflector. Fourier methods are then used to recover the reflected center wavelength of each grating.

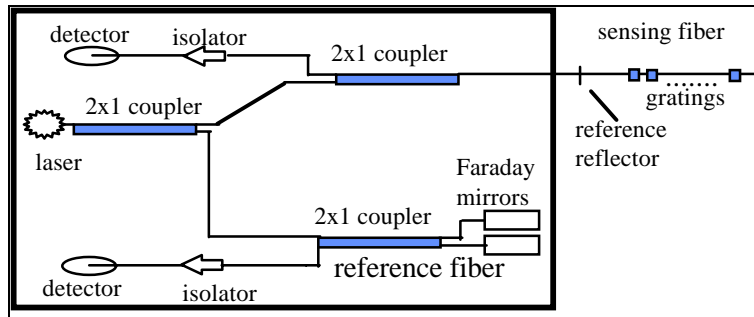


Figure 7. Schematic of demodulation system for optical network mounted on VME card(s).

To illustrate the FODSS system, strain measurements on a dual cantilever beam are presented in Figure 8. Twenty-two bragg gratings were distributed along a single fiber and the results were compared with resistance strain gauges. This type of strain measurement with optical fibers allows strain mapping of large structures such as aircraft aerodynamic surfaces to monitor the changing shape of morphing surfaces.

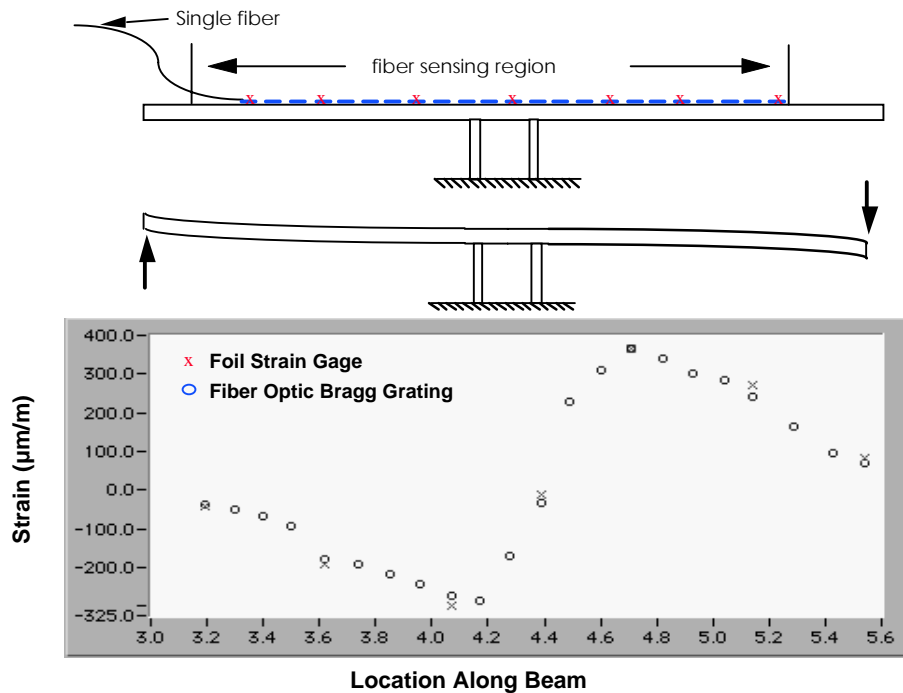


Figure 8. Strain measurement with Bragg gratings on cantilever beam.

5. FABRICATION OF INTEGRATED COMPOSITES

Interior noise and sonic fatigue are important issues in the development and design of advanced subsonic and supersonic aircraft. Conventional aircraft typically employ passive treatments, such as constrained layer damping and acoustic absorption material, to reduce the structural response and resulting acoustic levels in the aircraft interior. These techniques require significant addition of mass and only attenuate relatively high frequency noise transmitted through the fuselage. Adaptive and/or active methods of controlling the structural acoustic response of panels to reduce the transmitted noise may be accomplished with the use of SMA hybrid composite panels. These panels have the potential to offer improved thermal buckling/post buckling behavior, dynamic response, fatigue life, and structural acoustic response.

SMA's exhibit a characteristic phase transformation from martensite to austenite, initiating at the austenite start temperature and asymptotically ending at the austenite finish temperature. A SMA in the condition below the austenite start temperature, when plastically deformed and external stresses removed, will regain its original (memory) shape when heated. This phenomenon can be utilized to fabricate smart structures. The most common SMA is Nitinol (Nickel, Titanium, and Naval Ordnance Laboratory). The shape memory effect for this family of alloys is limited to nearly stoichiometric composition (Nickel: 53-57 wt%). Strains as high as 6-8% can be completely recovered by heating Nitinol above the austenite finish temperature. In addition, when Nitinol is heated, the Young's modulus increases three to four times and the yielding strength also increases approximately ten times.

Initial work in the fabrication of integrated composites has focused on the manufacture of E-glass/ Fiberite 934 epoxy panels with embedded shape memory alloys. Quasi-isotropic panels with unstrained SMA's embedded in the zero degree direction have been successfully fabricated. The lay-up of the panels fabricated is shown in Figure 9. Since 1/2 inch wide Nitinol strips were not available, five 0.10 inch wide, 5 mil thick rectangular Nitinol ribbons were butted together side to side with a spacing of 1/2 inch between sets. The SMA strips were heated to 250°F for an hour after

being cut and prior to being embedded to recover any initial strain that may have developed from being shipped wound on a spool. The SMA composite panels were processed using the standard 934 epoxy autoclave cure cycle (2hr @ 350°F, 100 psi). Test specimens machined from a cured hybrid panel are shown in Figure 10. Future panels will be fabricated with prestrained SMA strips. These panels will require tooling which will restrain the SMA strips from contracting during the thermal cure. Panels with bi-directional (0°/90°) SMAs as well as hybrid built-up structure will also be fabricated. All panels will be subjected to various tests to assess their noise, buckling, and fatigue characteristics as compared to baseline panels without embedded SMAs.



Figure 9. Schematic of shape memory alloy (SMA) hybrid composite beam lay-up.

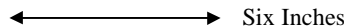


Figure 10. Test specimens machined from an E-glass/ 934 epoxy panel with embedded Nitinol shape memory alloy ribbons.

6. SUMMARY

A substantial amount of research is currently ongoing within the Materials Division at NASA LaRC to develop smart material technologies for active airframe systems. Research in the area of computer-aided design of materials has yielded computational models to predict the micromechanics of structural composites at elevated temperatures and to predict molecular orientation in high-temperature piezoelectric polymeric materials. Researchers are also developing two high-displacement piezoelectric actuator devices, RAINBOW and THUNDER. Current research on these actuators is focused on optimizing the piezoelectric performance and characterizing the fatigue life of such actuators. In the area of airframe health monitoring, fiber optic distributed strain sensors have been developed to measure strain in large-area structures. Research is also underway to develop arrays of such sensors to monitor the changing shape of airframe surfaces. Methods for fabricating composite components with sensor and actuator integration have also been developed. A majority of this research is being completed for specific applications including the fabrication of composite panels with embedded shape memory alloys for reducing sonic fatigue in aircraft structures.

7. REFERENCES

1. Wlezien, R. W., Horner, G. C., McGowan, A. R., Padula, S. L., Scott, M. A., Silcox, R. J., and Simpson, J. O., "The Aircraft Morphing Program", *Proceedings of the SPIE Smart Structures and Materials Symposium 1998*, Industrial and Commercial Applications Conference, Vol. 3326, Paper 3326-20, March 1998.
2. Gates, T.S., Chen, J.L., and Sun, C.T., "Micromechanical Characterization of Nonlinear Behavior of Advanced Polymer Matrix Composites," *Composite Materials: Testing and Design (Twelfth Volume)*, ASTM STP 1274, R.B. Deo and C.R. Saff, Eds., American Society for Testing and Materials, 1996, pp. 295-319.
3. Simpson, J.O., Ounaies, Z. and Fay, C., In Materials Research Society Proceedings: Materials for Smart Systems II, George, E., Gotthardt, R., Otsuka, K., Trolier-McKinstry, S., and Wun-Fogle, M., Ed., Materials Research Society: Pittsburgh, PA, Vol. 459, 1997.
4. Ounaies, Z., Young, J., Simpson, J.O., and Farmer, B., In Materials Research Society Proceedings: Materials for Smart Systems II, George, E., Gotthardt, R., Otsuka, K., Trolier-McKinstry, S., and Wun-Fogle, M., Ed., Materials Research Society: Pittsburgh, PA, Vol. 459, 1997.
5. G.H. Haertling, RAINBOW Ceramics - A New Type of Ultra-High-Displacement Actuator, *Am.Ceram.Soc.Bulletin*, 73, pp. 93-6, 1994.
6. M.W. Hooker, Properties and Performance of RAINBOW Piezoelectric Actuator Stacks, in Smart Materials and Structures 1997: Industrial and Commercial Applications of Smart Structures Technologies, *Proc. SPIE vol. 3044*, J.M. Sater, ed., Bellingham, WA: SPIE, pp. 413-420.
7. S.A. Wise, R.C. Hardy, and D.E. Dausch, Design and Development of an Optical Path Difference Scan Mechanism for Fourier Transform Spectrometers using High Displacement RAINBOW Actuators, in Smart Materials and Structures 1997: Industrial and Commercial Applications of Smart Structures Technologies, *Proc. SPIE vol. 3044*, J.M. Sater, ed., Bellingham, WA: SPIE, pp. 342-9.
8. Hellbaum, R.F., Bryant, R.G., Fox, R.L., Jalink, A., Rohrbach, W.W., and Simpson, J.O., Thin Layer Composite Unimorph and Ferroelectric Driver and Sensor, U.S. Patent 5,632,840, May 27, 1997.
9. Bryant, R.G., "Thunder Actuators", *5th Annual Workshop: Enabling Technologies for Smart Aircraft Systems*, NASA Langley Research Center, May 14-16, 1996.
10. Pinkerton, J.L. and Moses, R.W., "A Feasibility Study to Control Airfoil Shape Using THUNDER", NASA TM-4767, November 1997.
11. D.E. Dausch and S.A. Wise, "Compositional Effects on Electromechanical Degradation of RAINBOW Actuators", NASA-TM 206282, 1998.
12. D.E. Dausch, "Ferroelectric Polarization Fatigue in PZT-Based RAINBOWs and Bulk Ceramics", *J.Am.Ceram.Soc.* 80 [9], pp. 2355-60, 1997.
13. C.C. Hsueh, T. Tamagawa, C. Ye, A. Helgeson and D.L. Polla, Sol-Gel Derived Ferroelectric Thin Films in Silicon Micromachining, *Proc. 3rd Intl.Symp. on Integrated Ferroelectrics*, p. 231, 1991.
14. K.R. Udayakumar, S.F. Bart, A.M. Flynn, J. Chen, L.S. Tavrow, L.E. Cross, R.A. Brooks, and D.J. Ehrlich, Ferroelectric Thin Film Ultrasonic Micromotors, *Proc. 4th IEEE Workshop on Micro Electro Mechanical Systems*, p. 109, 1991.
15. M. Froggatt, "Distributed Measurement of the Complex Modulation of a Photoinduced Bragg Grating in an Optical Fiber," *Applied Optics*, Vol. 35, p 5162, 1996.

ACKNOWLEDGEMENTS

The authors would like to express our appreciation to the many people who have contributed their technical expertise and support to the research reported within this paper: Dr. Joseph Smith, Dr. John Connell, Mr. Harry Belvin, Mr. Mark Froggatt, Mr. Leland Melvin and Mr. Travis Turner of NASA Langley Research Center; Dr. Zoubeida Ounaies of the National Research Council; Dr. David Dausch of MCNC; Ms. Jennifer Young of University of Virginia; and Dr. Matthew Hooker of Lockheed-Martin Engineering and Sciences Company.